13th Australasian Fluid Mechanics Conference
Monash University, Melbourne, Australia
13-18 December 1998

INSTABILITY AND TRANSITION IN FLOW OVER A BACKWARD-FACING STEP

R. D. Henderson
Aeronautics & Applied Mathematics
California Institute of Technology, Pasadena, CA 91125, USA

D. Barkley and G. Gomez
Nonlinear Systems Laboratory, Mathematics Institute
University of Warwick, Coventry, CV4 7AL, UK

ABSTRACT

Computational linear stability results are presented for the flow over a backward-facing step with an expansion ratio (outlet height to inlet height) of two. The analysis shows that the first absolute linear instability of the steady two-dimensional flow is a steady three-dimensional bifurcation with wavelength 6.9 step heights at a critical Reynolds number of 748. Stability spectra and eigenmodes are presented for representative Reynolds numbers.

INTRODUCTION

The separated flow past a backward-facing step is important for several reasons. Firstly, separated flows produced by sudden changes in flow geometry are important in many engineering applications. This has been the practical motivation for many studies of backward-facing step flow over the past 30 years. Secondly, from a fundamental perspective, there is strong interest in understanding instability and transition to turbulence in non-parallel flows. Transition mechanisms in parallel flows such as plane channels and pipes have received substantial attention, and while many questions remain, these flows are considerably better understood than the non-parallel flows that arise in more complex geometries. The backward-facing step flow has emerged as a standard example of a simple yet nontrivial geometry in which to examine the onset of turbulence. Finally, from a strictly computational perspective, the two-dimensional flow over a backward-facing step is an established benchmark in computational fluid dynamics and therefore additional computational studies of this flow, such as the stability computations presented here, add important new information to the current database. Detailed knowledge of the three-dimensional structure and stability properties of flow over a backward-facing step in the transition range should be particularly important in defining the appropriate large-scale structure for large-eddy simulation combined with various turbulence models that may be used to simulate the flow at higher Reynolds numbers.

The two-dimensional linear stability of this flow has been examined extensively and is discussed in several publications [1–3]. However, additional computational evidence supports the existence of a local convective instability (again to two-dimensional disturbances) for a sizeable portion of the domain at $Re > 525$ [4]. In spite of the numerous investigations of flow over a backward-facing step available in the literature, two of the most basic questions for this flow remain open: in the ideal problem with no sidewalls, at what Reynolds number does the two-dimensional laminar flow first become linearly unstable, and what is the nature of this instability? These are the questions we wish to address.

FORMULATION

The flow is assumed to be governed by the incompressible Navier–Stokes equations, written in non-dimensional form as:

$$\frac{\partial \mathbf{u}}{\partial t} = \mathbf{N}(\mathbf{u}) - \frac{1}{\rho}\nabla p + \frac{1}{Re}\nabla^2 \mathbf{u} \quad \text{in } \Omega, \qquad (1)$$

$$\nabla \cdot \mathbf{u} = 0 \quad \text{in } \Omega, \qquad (2)$$

where $\mathbf{u}(\mathbf{x}, t)$ is the velocity field, ρ is the density, $p(\mathbf{x}, t)$ is the static pressure and Ω is the computational domain. $\mathbf{N}(\mathbf{u})$ represents the nonlinear advection term:

$$\mathbf{N}(\mathbf{u}) \equiv -(\mathbf{u} \cdot \nabla)\mathbf{u}. \qquad (3)$$

If the fluid is assumed to have constant density and constant dynamic viscosity μ, then the idealized flow depends on only three dimensional parameters: the kinematic viscosity $\nu = \mu/\rho$, and reference scales for length and velocity. Here we take as reference values the step height h and the maximum upstream centerline velocity U_∞. The only non-dimensional combination of these parameters gives the Reynolds number, $Re \equiv U_\infty h/\nu$, and this serves as the control parameter for the system.

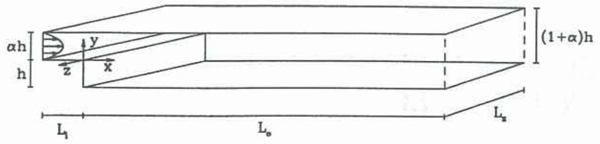

Figure 1: Flow geometry for the backward-facing step.

Figure 1 illustrates the computational domain under consideration and defines the geometric parameters for the problem. We take the edge of the step as the origin of our coordinate system. The computational domain has an inlet height αh and an outlet height $(1+\alpha)h$. In this study we fix $\alpha = 1$, giving an expansion ratio (outlet to inlet) of $1+\alpha = 2$. The inflow and outflow lengths L_i and L_o should be large enough that the results are independent of these parameters. At the inlet, $L_i = h$ is sufficient for the range of Reynolds numbers we consider [5,6]. The required outflow length L_o varies with Reynolds number and must be determined as part of a proper convergence study. Acceptable values for the range of Re considered here are $15h \leq L_o \leq 55h$ [7]. Finally we take the system to be infinitely large and homogeneous in the spanwise direction, i.e. $L_z = \infty$.

Boundary conditions are imposed as follows. At the inflow boundary ($x = -L_i$, $0 \leq y \leq \alpha h$) we impose a parabolic profile: $u = 4y(\alpha h - y)/(\alpha h)^2$, $v = w = 0$. Along the step and all channel walls we impose no-slip boundary conditions. At the outflow boundary ($x = L_o$, $-h \leq y \leq \alpha h$) we impose a standard outflow boundary condition for velocity and pressure:

$$\partial_x \mathbf{u}(\mathbf{x},t) = (0,0,0), \quad p(\mathbf{x},t) = 0.$$

Pressure is forced to satisfy a Neumann condition consistent with the momentum equation along all other boundaries [8].

COMPUTATIONAL METHODS

All of the calculations were carried out using a nonconforming spectral element method. In this method the domain Ω is represented by a mesh of K elements. Within each element the geometry and solution variables are interpolated using a tensor-product polynomial basis of order p in each direction, giving $N^2 = (p+1)^2$ grid points per element. Figure 2 shows the computational domains used for simulating the backward-facing step flow over the entire range of Reynolds number. Each grid uses local refinement to isolate the singularity induced by the sharp corner, and to resolve the recirculation zones in the wake of the step and along the upper wall. The use of local mesh refinement allows high-resolution of these critical flow regions while at the same time permitting the use of a large computational domain. A large domain size is required to isolate the region of interest from the effects of the outflow boundary.

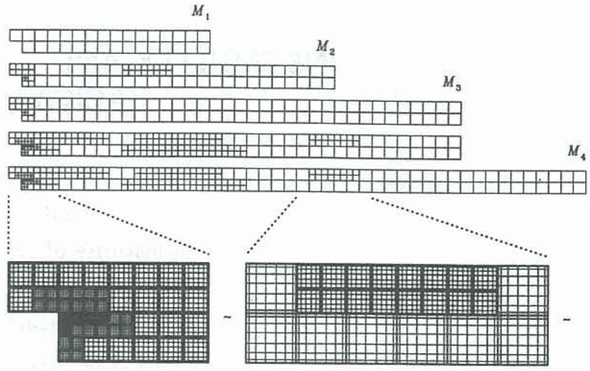

Figure 2: Computational domains for simulating flow over a backward-facing step. Two subsections of mesh M_1 are expanded to show the internal distribution of quadrature points for polynomial order $p = 7$.

Our computations consist of two parts. First we obtain steady two-dimensional solutions from either time-dependent simulations or Newton methods. Second we determine relevant bifurcation points along the steady branch of solutions via two- and three-dimensional linear stability analysis. The computational procedure is the same as that used previously [9,10]; here we only outline the essential features.

For the stability calculations we consider the evolution of a small perturbation $\mathbf{u}'$ to a steady base flow $\mathbf{U}$. Equations for the evolution of $\mathbf{u}'$ are obtained by replacing the nonlinear advection term in the Navier–Stokes equations with the linearization:

$$\mathbf{N}_{\mathbf{U}}(\mathbf{u}') \equiv -(\mathbf{u}' \cdot \nabla)\mathbf{U} - (\mathbf{U} \cdot \nabla)\mathbf{u}'.$$

Note that boundary conditions for the perturbation are the same as those for the base flow $\mathbf{U}$ except that $\mathbf{u}' = 0$ at the inlet.

Our primary concern here is the three-dimensional stability of steady two-dimensional flows. Because the system is homogeneous in the spanwise direction, we can decompose general perturbations into Fourier modes with spanwise wavenumbers β:

$$(\mathbf{u}', p')[x,y,z,t] = \int_{-\infty}^{\infty} (\hat{\mathbf{u}}, \hat{p})[x,y]\, \mathrm{e}^{\sigma t + \mathrm{i}\beta z}\, \mathrm{d}\beta.$$

In the linear approximation modes with different $|\beta|$ are decoupled. The Fourier components can be computed on a two-dimensional domain with β appearing in the linearized equations as an additional parameter. Our stability calculations therefore produce a family of eigenvalues $\sigma(\beta; Re)$ for a discrete set of fixed Reynolds numbers.

Note that by construction this approach determines the absolute, global stability properties of the

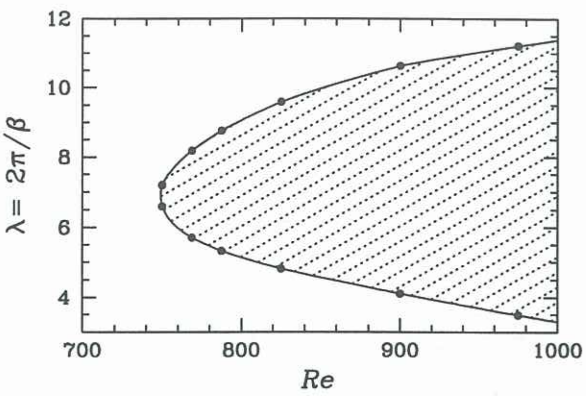

Figure 3: Neutral stability curve for the flow over a backward-facing step. Everywhere inside the shaded region there exist modes with positive growth rates.

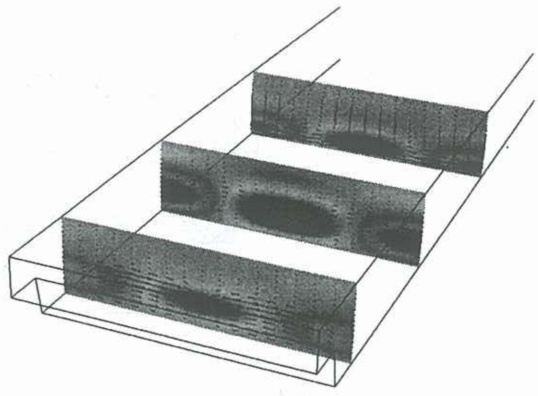

Figure 4: Three-dimensional structure of the leading eigenmode. Contours indicate the strength of the u-component of the perturbation and vectors indicate the spanwise flow pattern at each downstream plane.

flow. The functions $\phi[x, y, z] \equiv \hat{\mathbf{u}}[x, y] \exp(i\beta z)$ are the *global modes* of the system, and the eigenvalues $\sigma = \sigma_r + i\sigma_i$ are the corresponding *global frequencies.* A global instability is present if there is any mode with an *absolute growth rate* $\sigma_r > 0$.

Further details of the computational procedure along with a detailed convergence study for the set of parameters considered here are presented in [7].

RESULTS

We begin by presenting our findings for the dependence of eigenvalues on Reynolds number and spanwise wavenumber. Figure 3 shows the neutral-stability curve for the flow up to $Re = 1000$. Everywhere to the right of this curve there is a band of wavenumbers with $\sigma_r > 0$ and the flow is therefore linearly unstable to three-dimensional perturbations. The neutral stability curve becomes much more complicated for $Re > 1000$ because multiple eigenvalue branches cross the linear stability threshold. However, this occurs well above the primary instability. For this reason we have not attempted to resolve the eigenspectra in this more complicated regime.

Critical values for the flow were determined as follows. First, points along the neutral curve were obtained by accurately finding zero crossings of eigenvalue branches (as a function of β) for several Reynolds number between 750 and 1000. Next we computed a cubic fit to the neutral points near the tip of the curve. The critical values Re_c and β_c were then evaluated from the cubic fit, giving $Re_c = 748$ and $\beta_c = 0.91$ ($\lambda_c = 6.9$ step heights).

Note that the two-dimensional stability of the flow is determined by the structure of eigenspectra at $\beta = 0$. Our calculations indicate that all such eigenvalues satisfy $\sigma_r < 0$, and so the flow is two-dimensionally *stable* for $Re < 1000$. Preliminary results indicate that there may be a two-dimensional instability above $Re \approx 1350$, but the results so far are inconclusive. Further details about the behavior of the two-dimensional eigenspectra can be found in [7].

Now we turn to a description of the eigenmodes associated with the three-dimensional instability. The leading eigenmode at $Re = 750$ is shown in figure 4. The flow visualization is constructed by forming the linear superposition $\mathbf{U} + \epsilon\mathbf{u}'$ to produce a three-dimensional vector field. From the visualization we see that the instability takes the form of a flat roll that originate in the recirculation zone just downstream of the step. The size of the mode (wavelength and downstream extent) scales on the size of the primary recirculation zone. This length scale is much larger than either the step height h or the nominal thickness of shear layer separating from the step.

A more detailed view of the eigenmode structure of both the leading and secondary modes is shown in figure 5. Although in general σ is complex, the global frequency of the two leading modes is real ($\sigma_i = 0$) so they represent steady bifurcations. In this view we note that the primary instability mode has a large w-component both near the step and just upstream of the reattachment point on the lower wall. The secondary mode is linked with the recirculation zone on the upper wall but otherwise has the same qualitative structure, i.e. a flat roll structure that scales with the size of the recirculation zone.

From the visualization of the eigenmode we can determine that the primary linear instability does not arise either in the secondary recirculation zone or in the high-speed region between the primary and secondary recirculation zones. This rules out a Taylor-Görtler-type instability of the main flow as the source of three-dimensionality in experiments.

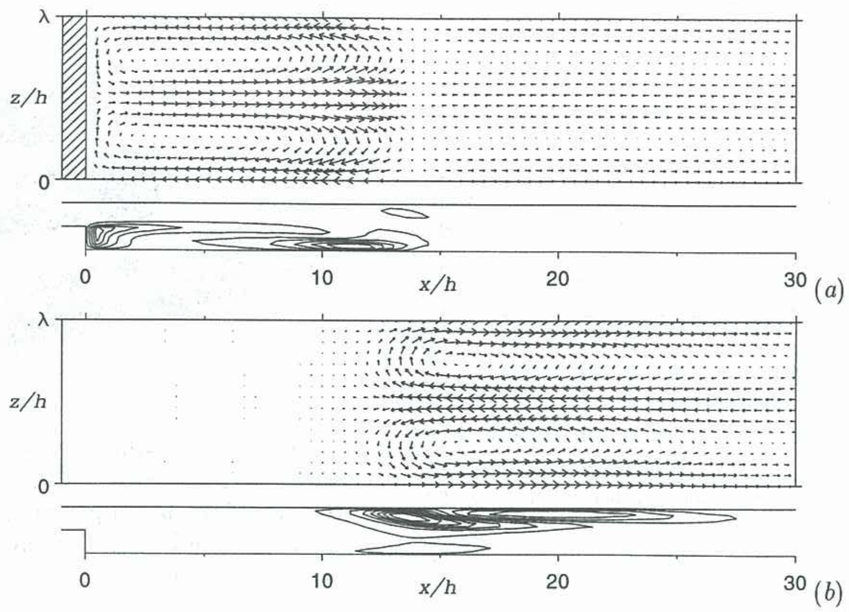

Figure 5: Structure of the global modes excited by perturbations to the backward-facing step: (a) leading mode (vector plot along $y = -0.65$); (b) secondary mode (vector plot along $y = 0.65$). The lower portion of each image shows $\hat{w}$-contours of the destabilizing Fourier mode. Note that both eigenmodes are real.

SUMMARY

We have shown that the primary bifurcation of the steady, two-dimensional flow over a backward-facing step with a 2:1 expansion is a three-dimensional instability. We have computed the critical Reynolds number and spanwise wavelength of the instability and find $Re_c = 748$ and $\lambda_c = 6.9h$. We have further determined the band of unstable wavenumbers for Re up to 1000. This data will be particularly useful in future numerical work as it allows the selection of appropriate spanwise domain lengths and sets the framework for detailed transition studies.

REFERENCES

[1] D. K. Gartling. A test problem for outflow boundary-conditions - flow over a backward-facing step. *Int. J. Numer. Meth. Fluids*, 11(7):953–967, 1990.

[2] P. M. Gresho, D. K. Gartling, J. R. Torczynski, K. A. Cliffe, K. H. Winters, T. J. Garratt, A. Spence, and J. W. Goodrich. Is the steady viscous incompressible 2-dimensional flow over a backward-facing step at Re=800 stable? *Int. J. Numer. Meth. Fluids*, 17(6):501–541, 1993.

[3] A. Fortin, M. Jardak, J. J. Gervais, and R. Pierre. Localization of Hopf bifurcations in fluid flow problems. *Int. J. Numer. Meth. Fluids*, 24(11):1185–1210, 1997.

[4] L. Kaiktsis, G. E. Karniadakis, and S. A. Orszag. Unsteadiness and convective instabilities in 2-dimensional flow over a backward-facing step. *J. Fluid Mech.*, 321:157–187, 1996.

[5] L. Kaiktsis, G. E. Karniadakis, and S. A. Orszag. Onset of 3-dimensionality, equilibria, and early transition in flow over a backward-facing step. *J. Fluid Mech.*, 231:501–528, October 1991.

[6] P. T. Williams and A. J. Baker. Numerical simulations of laminar-flow over a 3D backward-facing step. *Int. J. Numer. Meth. Fluids*, 24(11):1159–1183, 1997.

[7] D. Barkley, G. Gomez, and R. D. Henderson. Three-dimensional instability in flow over a backward-facing step. *J. Fluid Mech.*, 1998. *Submitted for publication.*

[8] G. E. Karniadakis, M. Israeli, and S. A. Orszag. High-order splitting methods for the incompressible Navier–Stokes equations. *J. Comput. Phys.*, 97(2):414–443, 1991.

[9] C. K. Mamun and L. S. Tuckerman. Asymmetry and Hopf bifurcation in spherical Couette flow. *Phys. Fluids*, 7(1):80–91, January 1995.

[10] D. Barkley and R. D. Henderson. Three-dimensional Floquet stability analysis of the wake of a circular cylinder. *J. Fluid Mech.*, 322:215–241, September 1996.